5th CIRP Global Web Conference Research and Innovation for Future Production

Quality assurance of brazed copper plates
through advanced ultrasonic NDE

Tiziana Segreto[a,b], Alessandra Caggiano[b,c], Roberto Teti[a,b]

aDept. of Chemical, Materials and Industrial Production Engineering, University of Naples Federico II, Piazzale Tecchio 80, 80125 Naples, Italy
bFraunhofer Joint Laboratory of Excellence on Advanced Production Technology (Fh J_LEAPT), Naples, Italy
cDepartment of Industrial Engineering, University of Naples Federico II, P.le Tecchio 80, 80125 Naples, Italy

* Corresponding author. Tel.: +393471337695; fax: +390817682362. E-mail address: tsegreto@unina.it

Abstract

Ultrasonic non-destructive methods have demonstrated great potential for the detection of flaws in a material under examination. In particular, discontinuities produced by welding, brazing, and soldering are regularly inspected through ultrasonic techniques. In this paper, an advanced ultrasonic non-destructive evaluation technique is applied for the quality control of brazed copper cells in order to realize an accelerometer prototype for cancer proton therapy. The cells are composed of two half-plates, made of high conductivity 99.99% pure copper, brazed one on top of the other. Full volume ultrasonic scanning based on the pulse-echo immersion testing method were carried out to allow for the ultrasonic 2.5 D axial tomography of the cell, realizing the quality assessment of the brazing process.

1. Introduction

Brazing is a key technology in the production of components made of high performance materials. The brazing process joins two pieces of metal or alloy together through a third, molten filler metal or alloy. The joint area is heated above the melting point of the filler metal or alloy but below the melting point of the base metals or alloys to be joined. The molten filler metal or alloy flows into the gap between the two metal pieces by capillary action and forms a strong metallurgical bond as it cools down to solidification. Brazed joints have high tensile strength, typically higher than the strength of the utilized filler metal or alloy [1].

The inspection of the assembly part constitute the last step of the brazing process and is essential for ensuring satisfactory quality of the whole brazed unit [2]. The main testing methods to disclose one or more types of brazing defects are divided into destructive and non-destructive testing (NDT) techniques [3]. Destructive methods such as peel tests, impact tests, and metallographic examination, are employed to ascertain whether a brazing design meets the specified requirements and are utilized for random or specific testing of brazing joints [4].

In industrial production, whenever it is necessary to inspect all fabricated components due to stringent safety requirements, there is a strong demand for quality assurance based on NDT methods [5].

An established method for NDT is ultrasonic (US) testing in pulse-echo mode [6]. In the case of brazed parts, this method allows to detect discontinuities in the brazing interface, such as voids and porosities, caused by inhomogeneous wetting by the filler metal of the pieces to be brazed.

In this paper, an advanced US non-destructive evaluation (NDE) technique based on full volume (FV) ultrasonic scanning [7, 8] is applied for the quality control of brazed copper cells of an accelerometer prototype utilized for radionuclide production and proton therapy use. The brazed cells consist of two plates, made of high conductivity 99.99% pure copper. The quality of the brazing process is critical for

the functionality of the prototype accelerator that does not contain any continuity solution in its structure in order to guarantee the homogeneity of the generated magnetic field responsible for protons acceleration.

The brazed back-to-back cell was scanned through FV US NDE allowing for 2.5 D US axial tomography. The quality assessment of the brazing process was carried out through multiple US image analysis.

2. Advanced ultrasonic non-destructive evaluation

The era of modern US techniques started about 1917 with Langevin's use of high-frequency acoustic waves and quartz resonators for submarine detection [9]. Underwater detection systems were developed for submarines navigation in World War I and in particular after the tragic sinking of the Titanic in 1912 for the detection of underwater icebergs.

In 1928, the Soviet scientist Sergei Y. Sokolov proposed a through-transmission technique for flaw detection in metals [10]. In this technique, he showed that flaws in metals could be detected by monitoring ultrasonic energy transmitted across the metal itself. However, the resolution of his experimental device was poor but the Sokolov's technique remains the basis of the modern US non destructive testing techniques [11].

The first flaw detecting device and measuring instrument was patented by Floyd Firestone [12] but the turning point was given by the introduction of piezoelectric crystal transducers by James F. McNulty for US testing [13].

Since that time, the field of US non- destructive evaluation (NDE) has grown enormously, with applications found in science, industry, medicine and other areas.

In modern manufacturing, US NDE methods are utilized for the detection of surface, subsurface and internal flaws (e.g. cracks, laminations, cavities, pores, inclusions, bonds, etc.) in different types of materials (e.g. metals, composite materials, plastics) [7, 14, 15]. In all major industries, US NDE techniques are largely used for quality control and materials inspection.

3. Prototype proton linear accelerator

The most direct way that particle accelerators influence most of our lives is through their applications in medicine. In the last decades, the use of energetic proton beams for deep seated cancer therapy is well settled and applied [16]. Worldwide, more than 30,000 patients have been treated with protons for various cancers and other diseases. In recent years, there has been a massive growth in the development of proton therapy centers in Canada, Japan, China, France, Germany, Switzerland, Italy and other countries already plan to build such centers (Poland, Hungary, Austria, Russia, Australia).

Since 2002, in Italy, a new proton linear accelerator centre consisting of two accelerators connected in cascade was designed and developed for radionuclide production and cancer therapy [17].

The configuration of the accelerator centre is based on a sequence of different acceleration stages, each of which acts as an injector for the consecutive one (Fig. 1). The structure of the prototype proton linear accelerator consists of three main devices:
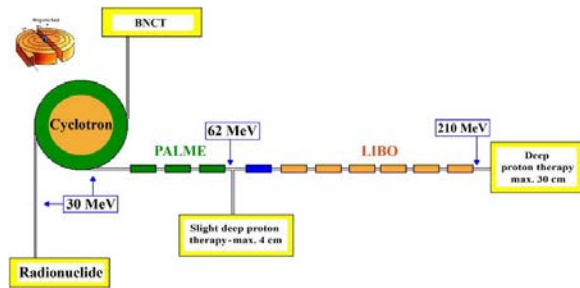

Fig. 1. Acceleration state scheme.

Fig. 2. . OHFC 99.99% copper half-cell plates showing a coupling half-cell (left) and an accelerating half-cell (right).

- a commercial cyclotron capable to generate energy up to 30 MeV, directly usable for the production of radionuclides employed for imaging or for the boron neutron capture therapy (BNCT);
- a first linear accelerator (Linac) with final energy 62 MeV, used directly for slight deep proton therapy (shallow tumors (max 4 cm) such as uveal melanoma);
- a second Linac with generated energy up to 210 MeV, for deep proton therapy (max 30 cm).

The first level of acceleration from 30 MeV to 62 MeV is called post linear accelerator of medium energy (PALME), and the second level of acceleration is called LIBO (Linac Booster) with a maximum amplified energy equal to 210 MeV. The latter was under study for this paper.

3.1. Linear accelerator LIBO

LIBO is a side-coupled Linac (SCL) operating at high radio frequency (RF) of 3 GHz [18]. This high frequency implies a Linac more compact and shorter than the standard lower-frequency proton Linacs utilized as injector of most synchrotrons. LIBO is composed of basic units, called modules and each one is fed by its own RF chain grouped into tanks. All LIBO modules are essentially identical, except for their gradual increase in length, corresponding to the increasing velocity of the protons.

Three elements are at the basis of the accelerating structure: the half-cell-plate, the bridge coupler and the end cell. A SCL consists of a bi-periodic chain of cavities (accelerating and coupling cells) coupled magnetically through appropriate holes. The diameters of the holes is designed in order to allow the particles passage and ensure the shunt impedance, the

resonance frequency as well as the coupling factor between the cavities. The accelerating cavities are aligned with the longitudinal propagation direction of the particles, while the coupling cavities are placed off-axis in order to notably reduce the size of the accelerator. The structure is designed so that the longitudinal electric field is in opposition phase to the adjacent accelerating cavities, and is practically zero in the coupling cavities.

In a RF Linac accelerator, the most important condition to be satisfied is the synchronization between the accelerating field and the particles. Thus, the longitudinal dimension of the cavities of the diverse tanks must adapt to the increasing particles velocity.

3.2. Material and brazing process

The back-to-back brazed cells, that are the basic building blocks of a tank, are made up of two rectangular plates with same in-plane size, 208 mm x 114 mm, and two different thickness values: the thicker plate, of thickness 12.6 mm, acts as the accelerating cell and, on the reverse side, the thinner plate, of thickness 5.0 mm, acts as the coupling cell (Fig. 2).

The half-cell plates are made of forged oxygen free high conductivity (OHFC) 99.99% copper with the following characteristics: high ductility, excellent electrical and thermal conductivity, high impact strength, good creep resistance, ease of welding, and low volatility under high vacuum.

All the half-cell plates were machined on CNC turning and milling machines. The pre-machined half-cell plates were stress-relieved in air at 250°C in order to guarantee, after the final machining operation, the high planarity required for vacuum brazing of the back-to-back cell.

Insertion of the brazing alloy was performed in a clean room under laminar air flow. Brazing was carried out at four temperature levels, ranging between 750° and 850° C, in an all-metal vacuum furnace. Two methods were used to apply the brazing alloy: standard silver-based alloys in the form of wires positioned in pre-machined grooves, and in the form of foils. The copper structure is fixed on a precisely machined steel girder to insure the necessary rigidity.

After the brazing process, the OHFC 99.99% copper back-to-back brazed cells reported in Fig. 3 where obtained. In Fig. 4, four back-to-back brazed cells are assembled in order to realize a tank of the LIBO proton accelerator.

4. Ultrasonic non-destructive testing

The advanced US NDE technique applied to the back-to-back brazed cell with a total thickness of 17.6 mm (12.6 mm thickness for the accelerating plate and 5.0 mm thickness for the coupling plate) was based on a pulse-echo US scanning technique in water through the use of a focused immersion US probe [8, 11].

4.1. Ultrasonic NDE system

To achieve the quality assessment for the brazing process of the back-to-back cell, an US NDE system with a specially designed hardware and custom made software (RoboTest© v.2.0, developed in LabView©) was utilized. The system was

developed at the Fraunhofer Joint Laboratory of Excellence on Advanced Production Technology, Naples, Italy [19]. A full volume (FV) US scanning procedure based on complete US waveform acquisition allowing the 2.5 D US axial tomography of the back-to-back brazed cell was applied. The hardware configuration of the advanced US NDE system is shown in Fig. 5 and consists of [8]:

- Oscillator/detector for US probe excitation and returning signal detection
- Transmitter/receiver focused high frequency US immersion probe for pulse-echo testing
- Digital oscilloscope connected to the oscillator/detector and to PC through a general purpose interface bus (GPIB)
- Mechanical handling system consisting of a 6-axis Staübli RX 60 L robotic arm (with a robot controller CS 7B) for the US probe displacement
- PC for US waveform acquisition and processing as well as US probe displacement control

Fig. 3. OHFC 99.99% copper back-to-back cell after the brazing process
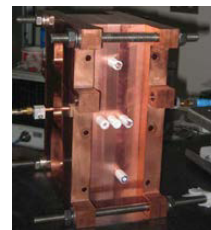

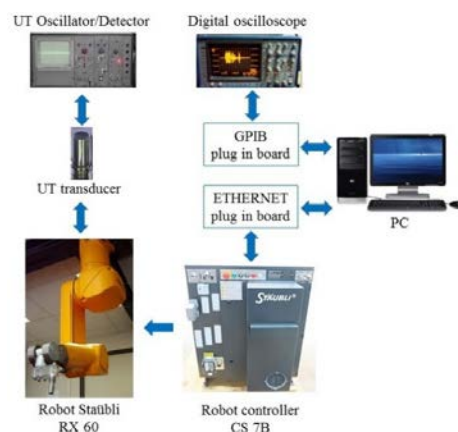Fig. 4. Assembly of the back-to-back accelerating cells

Fig. 5. Ultrasonic NDE system.

The custom made software code RoboTest© v.2.0 is capable to control the displacement of the UT NDE robotic system and provide for UT waveform signal detection, storage and analysis.

4.2. Ultrasonic NDE scanning procedure

Two pulse-echo immersion FV US scans were executed on the back-to-back brazed cell. The first scan was performed so that the US material interrogation was carried out from the surface of the 12.6 mm thick half-plate. The second scan was executed so that the US material interrogation was carried out on the reverse side, i.e. from the surface of the 5.0 mm thick half-plate. The parameters utilized for the FV US scans were the following (Table 1):

- Focused (25 mm focal length) high frequency (25 MHz) highly damped immersion US probe with scan step 1 mm
- Oscillator/detector set at 90 dB gain and medium damping
- Digital oscilloscope with 100 MHz sampling frequency, resulting in 500 samplings for each detected US waveform

For each probe position, during X-Y raster scanning of the back-to-back brazed cell, the entire US waveform was detected and digitized. A volumetric file was created and stored containing the entire set of digitized US waveforms for each material interrogation point during scanning.

5. Ultrasonic image generation

At the end of each FV US scan, from the acquired US volumetric file it is possible to obtain US images of any thickness portion of the cell under examination, allowing for 2.5 D US axial tomography of the back-to-back brazed cell.

The volumetric file consists of a matrix reporting the number of steps in the X direction, the number of steps in the Y direction and the digitized full US waveform in the Z direction (thickness direction) for each material interrogation point. These data can be processed to generate US images with grey tones or pseudo colours. A 256 grey tone scale was set up by using the minimum and maximum peak amplitude value in the volumetric file matrix as the 0 (black) and 255 (white) values in the grey scale.

Using the RoboTest© sub-module "Ecus Inspection", US images of any thickness portion of the part can be generated by positioning a time gate on the typical US waveform from the full volume US database. The time gate width identifies the material portion from which the US image is obtained.

In Fig. 6, the first screenshot of the "Ecus Inspection" sub-module is shown. In this window, information about the set-up of the executed US scan is reported (part size, scanning step, number of acquired US waveforms, etc.) together with the function for modifying/improving the US image visualization (image colours, image size, etc.). In the upper left, a 2D representation of the scanned back-to-back cell is shown. By clicking on the 2D representation with the red cursor, the US waveform for any material interrogation point of the part under examination is selected, retrieved from the volumetric file, and visualized in a plot reporting the US amplitude in 256 values scale vs. number of signal samplings.

The function "Change Limits" allows to generate a new plot where the selected US waveform amplitudes are reported in Volts (Y-axis) versus the US the time-of-flight (ToF) in seconds (X-axis). In this new US waveform graph, two sliders, represented by two movable vertical red lines, are utilized to set the time gates on the US waveform for the generation of US images.

The number of US images that can be simultaneously generated range from 1 (single image) to 16 (multi images). As the time axis orientation corresponds to the US propagation in the back-to-back cell thickness direction, the time gate or sub-gate width identifies the material thickness portion to be visualized. One image is generated for each sub-gate and each image represents the internal structure of the corresponding thickness portion of the back-to-back cell material.

6. Ultrasonic NDE results

The quality assurance of the brazed joint of the back-to-back-cell was carried out on the basis of the two FV US scans executed from both sides of the back-to-back cell: 12.6 mm thick half-plate and 5.0 mm thick half-plate.

Through the "Ecus Inspection" sub-module, for each FV US scan multiple US images were generated.

Table 1. Pulse-echo immersion FV US scanning data.

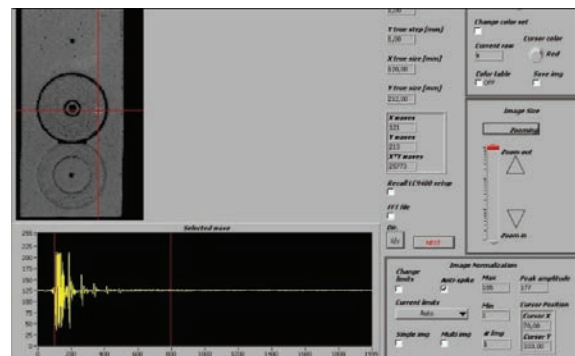| Scanning area (X-Y) [points]	Focal distance [mm]	Scanning step [mm]	US probe [MHz]	Inspection side
212x120	25	1	25 MHz	12.6 mm
212x120	25	1	25 MHz	5.0 mm

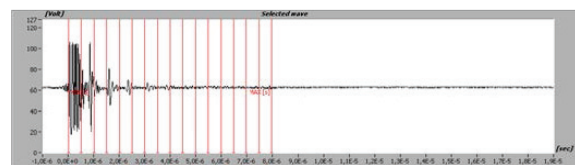Fig. 6. Ecus Inspection module: US image generation procedure.

Fig. 7. Selected US waveform with the 16 sub-gates for the multiple US image generation.

5.1. Results of FV US scan from the 12.6 mm inspection side

Fig. 7 reports the typical US waveform for the volumetric file of the FV US scan from the 12.6 mm inspection side (Table 1). To verify the quality of the brazed joint, 16 multiple US images were generated by setting a time gate of the entire US waveform and dividing it into 16 sub-gates.

Fig. 8 shows the obtained 16 US images where each image corresponds to 1.1 mm material portion of the back-to-back cell, i.e. 1/16 of the back-to-back cell thickness of 17.6 mm.

The 1st US image corresponds to the US waveform entering the back-to-back cell after travelling in water and shows the two circular features machined on the front surface. In the 2nd US image, besides the two circular features machined on the front surface, also the circular feature machined at 2 mm depth from the front surface. The 3rd and 4th US images evidence the geometry of the upper two circular features while the lower circular feature tends to disappear. The US images from 5th to 9th represent the US waveform passage through almost the entire thickness of the 12.6 mm half-cell. The US waveform interaction with the brazed joint layer is highlighted in the 10th, 11th and 12th US images.

As regards the evaluation of the quality of the brazed joint, the US image to be analyzed in detail is the 11th image that corresponds to a material layer in the thickness direction starting at 12.1 mm depth and finishing at 13.2 mm depth from the front surface of FV US scan. This material layer certainly includes the brazed joint which is located at 12.6 mm depth from the front surface. The US image shows the presence of a brazing defect at the upper side to the cell (11th image) indicated by a dark area, and highlighted in the figure with a red circle. No other brazing defect is visible in this image because of the difficulty of inspection due to the presence of the several circular geometry features located at different thickness levels in the back-to-back cell.

5.2. Results of FV US scan from the 5.0 mm inspection side

In order to clarify the possible presence of further brazing defects covered by the circular geometry features, a FV US scan was carried out from the 5.0 mm inspection side of the back-to-back cell (Table 1). The US image generated with reference to the brazed joint layer from the volumetric file of this FV US scan is reported in Fig. 9 both as 2D and 3D representation.

By examining the 2D US image, it is possible to verify the presence of the same brazing defect on the upper side of the cell but also a further defective area is now evidenced immediately under the central circular feature. This latter defective area could not be visualized through the previous FV US scan because of the coverage effect due to the presence of the circular geometry features in the back-to-back cell.
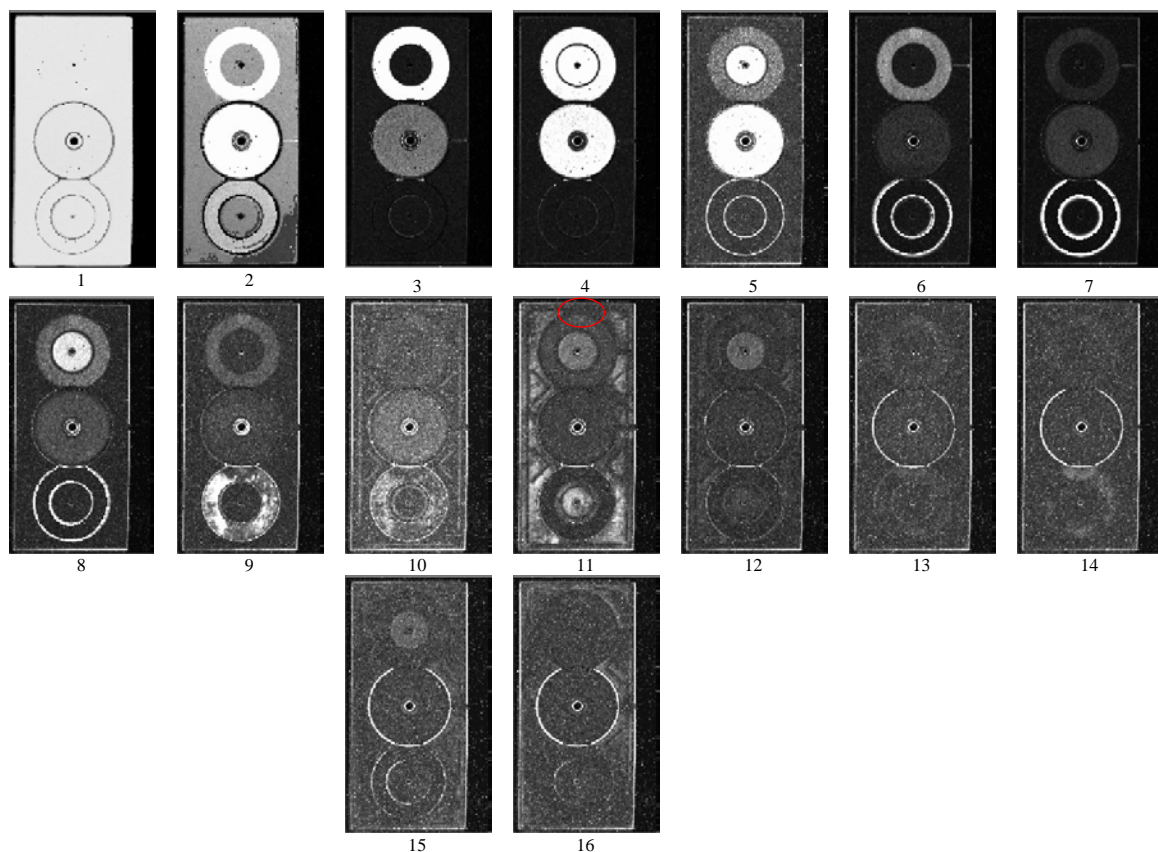

Fig. 8. Sequence layer by layer in the 12.6 mm side scan. Image 11 is characteristic for the brazed joint layer inspection between the copper plates.
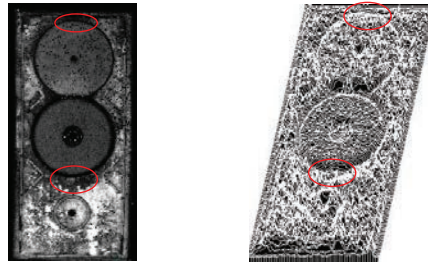
Fig. 9. 5.0 mm side US image of the brazing interface and 3D model of the scan.

7. Conclusions

An advanced ultrasonic NDE technique based on the FV US scanning technique was applied for the quality control of brazed copper cells of an accelerometer prototype utilized for radionuclide production and proton therapy use. The quality of the brazing process is critical for the functionality of the prototype that does not contain any continuity solution in its structure in order to guarantee the homogeneity of the generated magnetic field responsible for protons acceleration. The back-to-back cell consist of two half-cell plates, made of high conductivity OHFC 99.99% copper, brazed one on top of the other.

An US NDE system consisting of a specifically designed hardware configuration based on robotic probe displacement and a custom made software code was utilized for FV US scanning of the back-to-back brazed cell. Pulse-echo immersion FV US scans were executed using a focused high frequency immersion US probe from the two sides of the back-to-back brazed cell. The FV US scanning is based on the complete US waveform acquisition, allowing a 2.5 D US axial tomography of the part under examination.

Using the custom made software, US 2D images for any thickness portion of the back-to-back brazed cell were generated in order to assess the quality of the brazed joint.

The results obtained from the FV US scan executed from the 12.6 mm inspection side indicate a brazing defective area at the upper side of the cell. By examining the 2D US image obtained from the FV US scan carried out from the 5.0 mm inspection side, a further defective area was found immediately under the central circular feature of the cell.

The proposed FV US scanning procedure has the notable capability to carry out US NDE of the brazed joint from the 12.6 mm inspection side, traversing a material thickness of highly attenuating pure copper as large as 17.6 mm.

However, in order to obtain a thorough US NDE of the brazed joint, it has been necessary to carry out a double FV US scanning from both the 12.6 mm and the 5.0 mm inspection sides in order to be able to visualize additional brazing defects covered by the circular geometry features machined in the back-to-back cell.

The US NDE technique, utilized in this paper, has allowed replacing the back-to-back cells with brazing defects before they were grouped to form the accelerating structure of the LIBO.

References

[1] Schwartz MM. Brazing 2nd Edition. ASM International; 2003.
[2] Vollaro MB. Evaluation and quality control of brazed joints. ASM Handbook: Welding, Brazing, and Soldering (ASM International) 1993; 6: 1117- 1123.
[3] Campbell FC. Inspection of metals: understanding the basics, ASM International; 2013.
[4] McCall JL, French PM. Metallography as a quality control tool. Springer; 1980.
[5] Shull PJ. Nondestructive evaluation: theory, techniques, and applications. CRC Press; 2002.
[6] Blitz J, Simpson G. Ultrasonic methods of non-destructive testing. Springer; 1995.
[7] Teti R. Ultrasonic identification and measurement of defects in composite material laminates. CIRP Annals 1990; 39/1: 527-530.
[8] Segreto T, Bottillo A, Teti R. Advanced ultrasonic non-destructive evaluation for metrological analysis and quality assessment of impact damaged non-crimp fabric composites. Procedia CIRP 2016; 41: 1055-1060.
[9] Graff KF. A history of ultrasonics, in Physical Acoustics, XV, Academic Press, New York, 1982.
[10] Sokolov S, Phy. Z. 36 (142), 1935 and Techn. Physic USSR 2, 522, 1935.
[11] Peter J. Shull, Non destructive evaluation: theory, techniques, and applications, CRC Press, 2002.
[12] Firestone FA. Patent n. US 2280226A. Flaw detecting device and measuring instrument, 1942.
[13] Mcnulty JF. Patent n. US3260105A. Ultrasonic testing apparatus and method, 1966.
[14] Casperson R, Knöppchen A, Pohl R, Zimne L, Bode J. Manufacturing of reference defects for NDT using low-energy EDM. Procedings of 19th World Conference on Non-Destructive Testing 2016; 1-10.
[15] Alobaidi WM, Al-Rizzo HM, Sandgren E. NDT applied to the detection of defects in oil and gas pipes: a simulation-based study. ASME 2015 Int. Mech. Eng. Congr. Expo. 2015; 2B: Advanced Manufacturing.
[16] DeLaney TF, Haas RL. Innovative radiotherapy of sarcoma: proton beam radiation. Eur J Cancer, 2016; 62:112-123.
[17] Amaldi U, Berra P, Crandall K, Toet D, et al. LIBO—a linac-booster for protontherapy: construction and tests of a prototype. Nuclear Instruments and Methods in Physics Research A, 2004; 521:512-529.
[18] De Martinis C et al. Acceleration tests of a 3 GHz proton linear accelerator (LIBO) for hadrontherapy. Nuclear Instruments and Methods in Physics Research A, 2012; 681:10-15.
[19] http://www.jleapt-unina.fraunhofer.it/